**Preprints of the 21st IFAC World Congress (Virtual)**
**Berlin, Germany, July 12-17, 2020**

# On the Optimization of the Semi-Active Suspension for a Railway Vehicle

**Aslı Soyiç Leblebici** * **Semiha Türkay** **

* *Mechatronics Program, Eskisehir Osmangazi University, Eskisehir, Turkey, (e-mail: aleblebici@ogu.edu.tr).*
** *Electrical Engineering Department, Eskisehir Technical University,Eskisehir, Turkey (e-mail: semihaturkay@eskisehir.edu.tr)*

**Abstract:** In this study, a nine-degrees-of-freedom full wagon railway model with linear parameters is used to study the vehicle's vibrational response on the random rail data collected by Turkish State Railways Research Center (TCDD-DATEM). The performance of suspension system is determined by comparing the body vertical, pitch and roll accelerations, and suspension travels to assess ride comfort and handling properties of the vehicle. The semi-active suspension system is designed for three different controllers;*skyhook, groundhook and hybrid* since these approaches feature simplicity and lower cost compared to their active counterparts. For the proposed controllers, their effectiveness is validated by simulation results performed in MATLAB by comparing the achieved time responses.

*Keywords:* Railway vehicle, skyhook control, groundhook control, hybrid design, multi-objective control.

## 1. INTRODUCTION

The urgency to achieve a better compromise between the conflicting requirements of the railway vehicle has been leading to several new advancements in the vehicle suspensions. The suspension systems may ensure better comfort by optimized passive suspensions (Leblebici and Türkay, 2016), design of semi-active controllers or their active configurations, (Hohenbichler et al., 2006). A passive suspension is made up of components with fixed characteristics where the ride comfort, suspension deflection and rail holding objectives can not be met simultaneously. However, this issue can be resolved by replacing the passive suspension with an active or a semi-active suspension.

Though active systems have been studied extensively by using different control methods (i.e. PID control, LQG control, adaptive control, multiobjective $H_2/H_\infty$ control), their applicabilities in operation are still very limited and expensive (Zolotas and Goodall, 2018), (Savaresi et al., 2003). However, since the semi-active damper (Karnopp et al., 1974) has the ability to change its damping characteristics by using a little amount of external power and provide controlled real-time dissipation of energy, it is cheaper and less complex compered to the active conterparts and more reliable when compared to the passive ones. Thus, the semi active suspension is becoming more and more popular for railway vehicles (Zheng, 2011), (Guglielmino et al., 2008). In (Foo and Goodall, 2000), not only the railway vehicle body vertical acceleration but also first bending mode of the car body is suppressed by using an electro-magnetic actuator. Although one can get getting better comfort levels with variable damping, in (Li and Goodall, 1999), it is shown that the on/off skyhook control may cause larger suspension deflections when the vehicle is exposed to deterministic track inputs. In (Hohenbichler et al., 2006), an optimal skyhook design is considered that can improve the passenger comfort while keeping the suspension deflection on the same level. Since the skyhook control is a real time method, in (Vassal et al., 2006) the problem is re-defined in the control-oriented framework and an optimal skyhook control algorithm is developed for a quarter vehicle model. In this paper, for a full car railway vehicle model, a real-time semi-active controller is designed by using *skyhook, groundhook* and *hybrid* methods. As a disturbance input, the vertical profile track irregularities measurements from Turkey Konya-Polatlı high speed mainline are used. The results are discussed in terms of the root-mean-square (rms) values performances and the vehicle output time responses.

This study is organized as follows: Section 2 includes a detail modelling of nine-degrees-of-freedom (9 DOF) railway vehicle. The corresponding discrete-time model is obtained for real-time controller design. In Section 3, the semi-active systems are explained and the skyhook, groundhook and hybrid controls are designed for the 9DOF railway vehicle model. The results are discussed in detail. The study is finished by the Conclusions section.

## 2. VEHICLE MODEL

The schematical representation of the 9 DOFe model for the Siemens ICE high speed train is shown in Fig. 1. In the figure, the car body ($m_c$) and the bogie mass ($m_t$) are assumed to be rigid and to be able to move in heave, pitch and roll directions with the displacements ($z_c,\ z_{ti}$), ($\theta_c,\ \theta_{ti}$), and ($\phi_c,\ \phi_{ti}$), respectively. Here $i = 1$ stands for the 'front', and $i = 2$ for the the 'rear' bogie of the wagon, while the 'right' and the 'left' bearings are indexed with $j = 1, 2$ consecutively. The secondary suspension at each connection point consists of an active control force $u_{ij}$ and

a linear pair $(k_2, c_2)$, whereas $(k_1, c_1)$ serves as a primary suspension excited with the rail input $z_{w(ik)}$ at each wheel $k$.

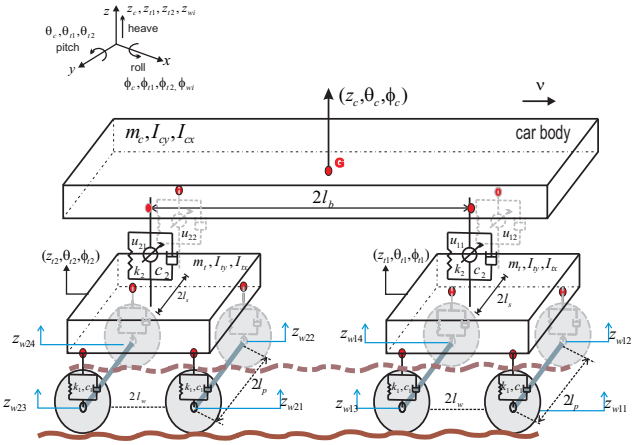


Fig. 1. The mathematical model of the wagon

Let's concatenate the displacements for the carbody and the sequential bogies into the vectors $x_c = [z_c\ \theta_c\ \phi_c]^T$ and $x_{bi} = [z_{ti}\ \theta_{ti}\ \phi_{ti}]^T$, for $i = 1, 2$, respectively. The nodal displacements highlighted with red bullets in Fig. 1 can be written overhand as:

$$\begin{aligned}
[\, z_{11}\ z_{12}\ z_{21}\ z_{22}\,]^T &= S_c x_c,\\
[\, z'_{11}\ z'_{12}\ z'_{21}\ z'_{22}\,]^T &= T_c S_c x_{b1} + T_t S_c x_{b2},\\
[\, z^p_{i1}\ z^p_{i2}\ z^p_{i3}\ z^p_{i2}\,]^T &= S_t x_{bi},
\end{aligned}$$

for

$$S_c = \begin{bmatrix} 1 & l_b & -l_s \\ 1 & l_b & l_s \\ 1 & -l_b & -l_s \\ 1 & -l_b & l_s \end{bmatrix}, \quad S_t = \begin{bmatrix} 1 & l_w & -l_p \\ 1 & l_w & l_p \\ 1 & -l_w & -l_p \\ 1 & -l_w & l_p \end{bmatrix},$$

$$T_c = \begin{bmatrix} 1/2 & 0 & 1/2 & 0 \\ 0 & 1/2 & 0 & 1/2 \\ 0 & 0 & 0 & 0 \\ 0 & 0 & 0 & 0 \end{bmatrix}, \quad T_t = \begin{bmatrix} 0 & 0 & 0 & 0 \\ 0 & 0 & 0 & 0 \\ 1/2 & 0 & 1/2 & 0 \\ 0 & 1/2 & 0 & 1/2 \end{bmatrix}.$$

Then, the dynamic forces for the secondary and primary suspensions shown with $F_{ij}$ and $F^p_{ik}$ respectively are expressed as,

$$\begin{aligned}
F_{ij} &= -k_2(z_{ij} - z'_{ij}) - c_2(\dot{z}_{ij} - \dot{z}'_{ij}) - u_{ij},\\
F^p_{ik} &= -k_1(z^p_{ik} - z_{w(ik)}) - c_1(\dot{z}^p_{ik} - \dot{z}_{w(ik)}),
\end{aligned} \tag{1}$$

and their equations of motion can be written disjointly as below:

▷ Secondary Suspension,

$$\begin{aligned}
m_c \ddot{z}_c &= \sum_{i=1}^{2}\sum_{j=1}^{2} F_{ij},\\
I_{cy}\ddot{\theta}_c &= \sum_{j=1}^{2} -l_b(F_{2j} - F_{1j}),\\
I_{cx}\ddot{\phi}_c &= \sum_{i=1}^{2} -l_s(F_{i1} - F_{i2}).
\end{aligned} \tag{2}$$

where $I_{cy}$ and $I_{cx}$ denote the pitch and roll moment of inertias of the car body.

▷ Primary Suspension,

$$\begin{aligned}
m_t \ddot{z}_{ti} &= \sum_{j=1}^{2} -F_{ij} + \sum_{k=1}^{4} F^p_{ik},\\
I_{ty}\ddot{\theta}_{ti} &= \sum_{j=1}^{2} +l_w(F^p_{ij} - F^p_{i(j+2)}),\\
I_{tx}\ddot{\phi}_{ti} &= \sum_{j=1}^{2}(-l_p(F^p_{i(2j-1)} - F^p_{i(2j)}) + \dots\\
&\quad + (-1)^{j+1} l_s F_{ij}),
\end{aligned} \tag{3}$$

likewise $I_{ty}$ and $I_{tx}$ denote the pitch and roll moment of inertias of the bogies.

Let's define a state vector $\tilde{x} = [x_c\ x_{b1}\ x_{b2}]^T$, a control input $u = [u_{ij}]^T$ and an exogeneous input $w = [z_{w(ik)}]^T$ for $i, j = 1, 2$, and $k = 1, ..., 4$. Then, the coupled system can bu put in the matrix form:

$$M\ddot{\tilde{x}} = \tilde{K}\tilde{x} + \tilde{C}\dot{\tilde{x}} + k_1\tilde{S}_t^T w + c_1\tilde{S}_t^T\dot{w} - (T\tilde{S}_c)^T u, \tag{4}$$

where

$$\begin{aligned}
M_c &= diag(m_c,\ I_{cy},\ I_{cx}),\\
M_t &= diag(m_t,\ I_{ty},\ I_{tx}),\\
M &= diag(M_c,\ M_t,\ M_t),\\
K_s &= diag(k_2 I_{12},\ k_1 I_8),\\
C_s &= diag(c_2 I_{12},\ c_1 I_8),\\
T &= [\, I_4\ -T_c\ -T_t\,],\\
T_s &= diag(-T^T T,\ -I_8),\\
\tilde{S}_c &= I_3 \otimes S_c,\\
\tilde{S}_t &= [\, 0_{8\times 3}\ I_2 \otimes S_t\,],\\
\tilde{S}_s &= [\, \tilde{S}_c^T\ \tilde{S}_t^T\,]^T,\\
\tilde{K} &= \tilde{S}_s^T K_s T_s \tilde{S}_s\\
\tilde{C} &= \tilde{S}_s^T C_s T_s \tilde{S}_s.
\end{aligned}$$

Here $diag(.)$ represents a diaogal matrix, $0_{m\times n}$ and $I_m$ denote respectively $m$ by $n$ null and $n$ by $n$ identity matrices, while $I \otimes S$ shows the Kronecker product of two given matrices $I$ and $S$. In this work, the suspension parameters tabularized in (Lei, 2017) are going to be used in the simulation studies in the subsequent sections.

### *2.1 Rail Track Measurements*

In this study, the high speed train is assumed to run on the Konya-Polath high speed rail line in Turkey with a constant speed of 200 $km/h$. Turkish State Railways Research Center (TCDD-DATEM) collects the data with Piri-Reis TRC which has the same specifications with high speed main line trains in service operation. According to the EN13848-1, for longitudinal level and alignment three different wavelength filters like as: $D_1 = 3m\ < \lambda \leq\ 25m$, $D_2 = 25m\ < \lambda \leq\ 70m$ and $D_3 = 70m\ < \lambda \leq\ 150m$. The relationship between wavelength and the frequency is defined with $Ff = v/\lambda$. Since the vehicle body modes occur under 1.2 $Hz$ in simulations as a disturbance input the $D_2$ filtered measurements that are shown in Fig. 2 are used.

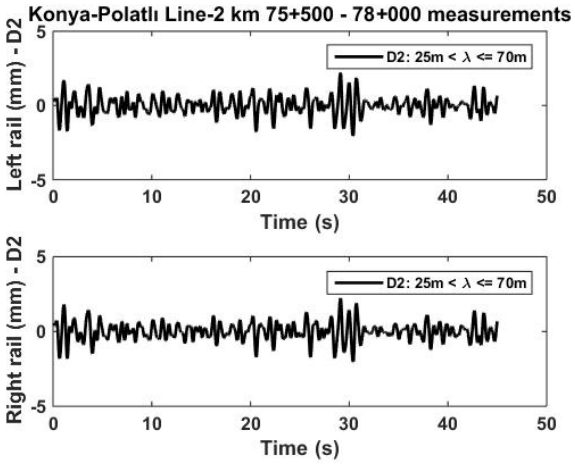


Fig. 2. Konya - Polatlı high speed main line records

In this study, the state space form has the disturbance input vectors $w$ and $\dot{w}$. Since the wheels displacements form the measurement vector $w$, the plant should be updated from wheels displacement vector $w$ to the output vector by re-defining the state vector as $\tilde{x} := x + B_{12}w$. The necessity conditions for conversion are;

- The A matrix should be full rank (invertible)
- The plant should be strictly proper

Then the new state-space equation is given in equation (5) with $B_1 = B_{11} + AB_{12}$.

$$\dot{\tilde{x}} = A\tilde{x} + B_1 w + B_2 u \tag{5}$$

## 3. SEMI-ACTIVE CONTROL

The main role of the semi-active systems is to ensure passenger comfort and safety by isolating body from the ground vibrations. In terms of performances, the semi-active systems are placed between passive and active systems. The semi-active suspension system base on the replacement of passive dampers with adjustable dampers, (Karnopp et al., 1974). The most commonly used semi-active algorithms are skyhook damping (for sprung mass), groundhook damping (for unsprung mass) and the hybrid control (a combination of skyhook and groundhook dampings).

The skyhook and groundhook damping semi-active control method is shown in Fig. 3. In the figure, $m_s$ denotes the sprung mass while $m_u$ refers to the unsprung mass. $F_{semi}$ is the semi-active force. The skyhook damper can be defined as the damper which is connected between the body and the sky as in Fig.3. This is not possible to realize physically, then this control algorithm can be explained by equation (6). The main idea is applying high damping to the sprung mass while the sprung mass and unsprung mass come close to or move away from each other. Since the force is directly related to the absolute velocity of the body it can also named as absolute damper.

$$F_{semi} = F_{sky} = \begin{cases} c_{sky}\dot{z}_b(t) & \dot{z}_b(t)\left(\dot{z}_b(t) - \dot{z}_t(t)\right) > 0, \\ 0 & \text{else} \end{cases} \tag{6}$$

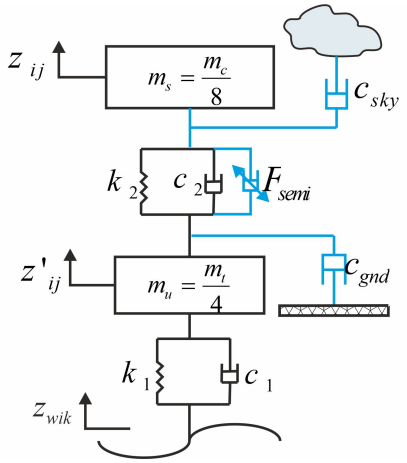


Fig. 3. Semi-active control

The groundhook damper similar to the skyhook damper is also a semi-active control element in vehicle dynamics. The main idea is connecting a value changeable damper between the unsprung mass and the ground as in Fig. 3 which could not be realized physically. It can be formulated as in equation (7). The behaviour can be explained as applying lower damping to the unsprung mass while sprung mass and unsprung mass come close to or move avay from each other. The expected performance is suppressing the unsprung mass body accelerations on the high frequencies.

$$F_{semi} = F_{gnd} = \begin{cases} c_{gnd}\dot{z}_t(t) & -\dot{z}_t(t)\left(\dot{z}_b(t) - \dot{z}_t(t)\right) > 0, \\ 0 & \text{else} \end{cases} \tag{7}$$

According to the equations, in on/off skyhook and groundhook damping algorithms, it should be monitored the absolute velocities of the sprung and unsprung masses and the relative velocities between sprung and unsprung masses for every time instances. Therefore, the corresponding discrete time state space equation should be obtained. In this study, for a sampling time $t_s$ the model in equation (5) was transformed into discrete timeby using zero-order-hold (zoh) method and given in equation (8).

$$\tilde{x}[k+1] = A^d\tilde{x}[k] + B_1^d w[k] + B_2^d u[k] \tag{8}$$

### *3.1 Skyhook Damping Control of Railway Vehicle*

In this study as a semi-active control design at first skyhook damping method is applied to the 9 DOF vehicle. The control inputs are designed in equation (10). It is assumed that all skyhook dampers have the same values to decouple the vehicle modes. The measurement vector is chosen as $y(t) = [\dot{z}_{ij}\ (\dot{z}_{ij} - \dot{z}'_{ij})]^T$ and the corresponding discrete time measurements are given in equation (9).

$$y[k] = C_{SKY}\tilde{x}[k+1] + D_{SKY1}w[k] \tag{9}$$

$$u_{ij} = \begin{cases} c_{sky}\dot{z}_{ij}(t) & \dot{z}_{ij}(t)\left(\dot{z}_{ij}(t) - \dot{z}'_{ij}(t)\right) > 0, \\ 0 & \text{else} \end{cases} \tag{10}$$

for $i, j = 1, 2$.

To determine the skyhook damper optimal value, the rms values of the car body vertical accelerations are calculated and plotted for $0 \leq c_{sky} \leq 100\ kNs/m$. The value 68 $kNs/m$ provides the minimum car body heave acceleration rms value but the car body roll acceleration rms value is above the passive value. Since the car body roll acceleration also has a significant effect on passenger comfort, the value of the skyhook damping is chosen as $c_{sky} = 26\ kNs/m$ that minimize the car body roll acceleration rms value. Figures 4-5 summarizes the skyhook damper value effects on vehicle outputs. The Figures 6-7 show the car body heave, pitch and roll accelerations ($\ddot{z}_c$, $\ddot{\theta}_c$, $\ddot{\phi}_c$ respectively) and the secondary suspension deflection ($s_{11}$) time responses. According to the figures the semi-actively controlled vehicle perform better than the uncontrolled vehicle.

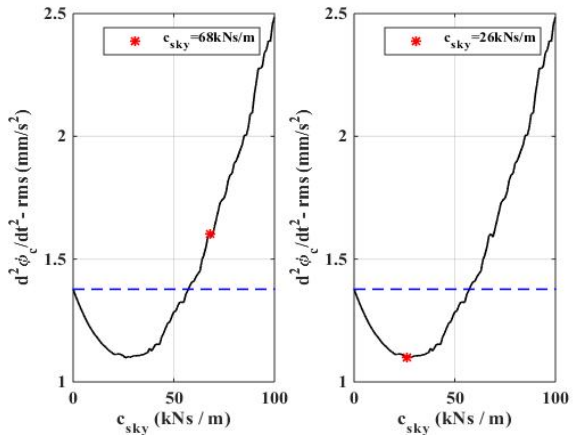


Fig. 4. Skyhook damping effects on car body roll acceleration rms value

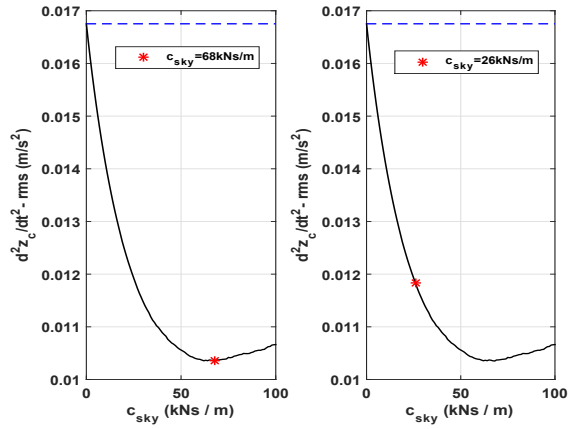


Fig. 5. Skyhook damping effects on car body vertical acceleration rms value

### *3.2 Groundhook Damping Control of Railway Vehicle*

In this study to design a groundhook damping for 9 DOF vehicle the measurement vector should be selected as $y(t) = [\dot{z}'_{ij}\ (\dot{z}_{ij} - \dot{z}'_{ij})]^T$ and the discretized form is given

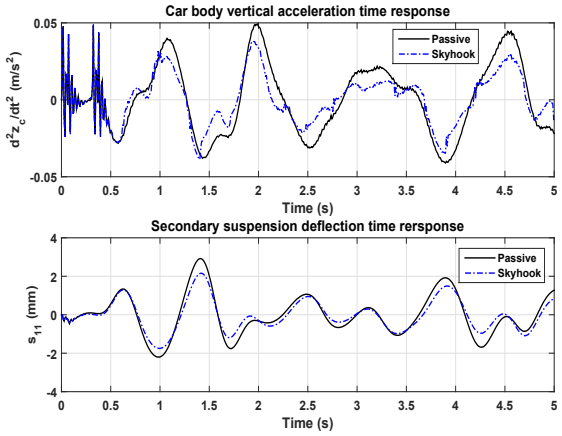


Fig. 6. The car body heave acceleration and the secondary suspension deflection time responses of the passive and semi-actively controlled vehicle.

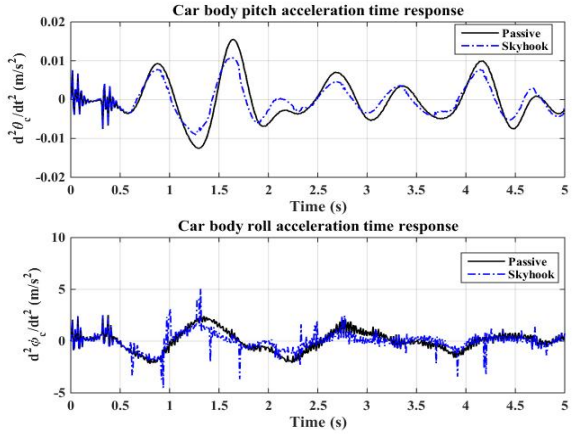


Fig. 7. The car body pitch and roll accelerations time responses of the passive and semi-actively controlled vehicle.

in equation (11). The control forces may be defined as in equation (12) for a single value of groundhook damper.

$$y[k] = C_{GND}\tilde{x}[k] + D_{GND1}w[k] \tag{11}$$

$$u_{ij} = \begin{cases} c_{gnd}\dot{z}'_{ij}(t) & -\dot{z}'_{ij}(t)\left(\dot{z}_{ij}(t) - \dot{z}'_{ij}(t)\right) > 0, \\ 0 & \text{else} \end{cases} \tag{12}$$

for $i, j = 1, 2$.

To determine the optimum groundhook damper value, for $0 \leq c_{gnd} \leq 100\ kNs/m$ the vehicle output rms values are calculated and plotted as in Figures 8-9. According to the figure, it is not possible to get smaller suspension deflections by using groundhook damping method. The value of the groundhook damper is fixed as $c_{gnd} = 24\ kNs/m$ which minimizes the car body heave acceleration rms value in defined range. The Fig. 10 and Fig.11 show the car body heave, pitch and roll accelerations ($\ddot{z}_c$, $\ddot{\theta}_c$, $\ddot{\phi}_c$ respectively) and the secondary suspension deflection ($s_{11}$) time responses. Although the groundhook provide better ride comfort than the passive system, the results are not sufficient as the skyhook damping.

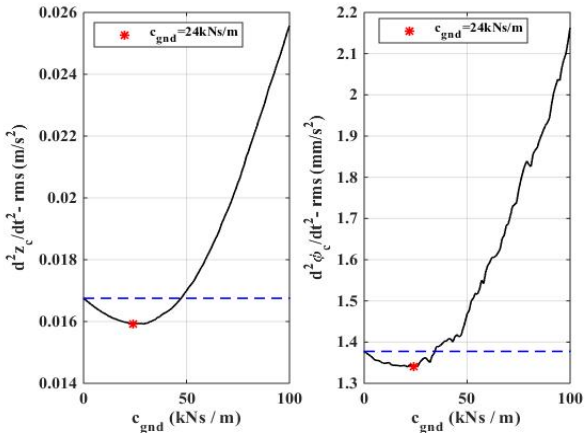


Fig. 8. The groundhook damping $c_{gnd}$ effects on the car body heave and roll accelerations rms values.

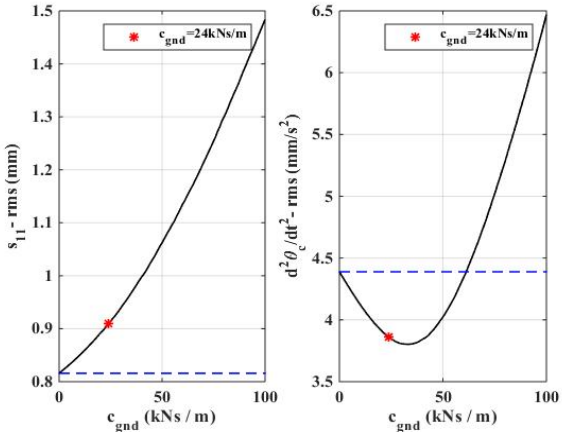


Fig. 9. The groundhook damping $c_{gnd}$ effects on the secondary suspension deflection and car body pitch acceleration rms values.

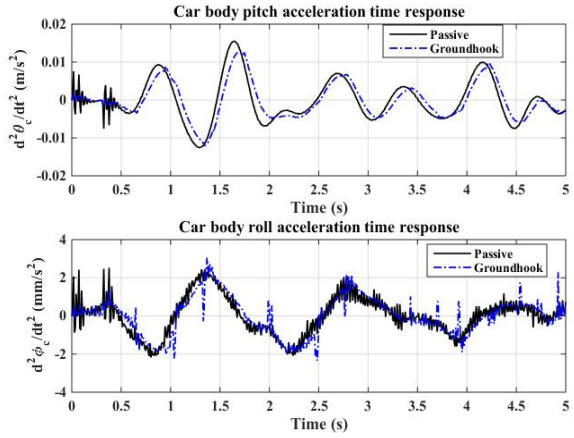


Fig. 10. The car body pitch and roll accelerations time responses of the passive and semi-actively controlled vehicle.

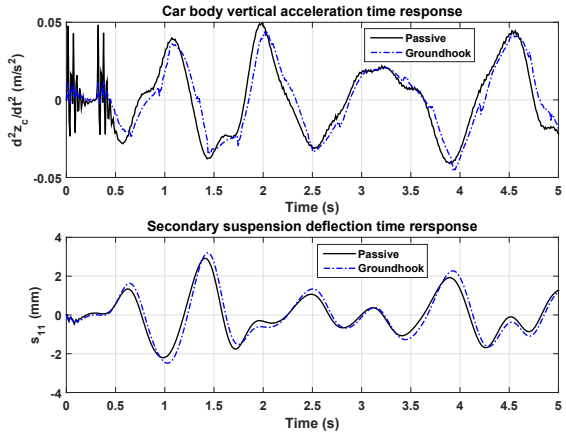


Fig. 11. The car body heave acceleration and the secondary suspension deflection time responses of the passive and semi-actively controlled vehicle.

### *3.3 Hybrid Control*

The hybrid control is a semi-active control algorithm which is a combination of skyhook and groundhook methods. It uses the advantages of both skyhook and groundhook dampers and defined as:

$$u_{ij} = G_{hyb}\left[\alpha \dot{z}_{ij} + (1-\alpha)\dot{z}'_{ij}\right] \tag{13}$$

where $G_{hyb}$ is a constant and $\alpha \in [0,1]$ is the ratio between skyhook and groundhook. If $\alpha$ is chosen as 0 the hybrid control equals to the skyhook damping while $\alpha = 1$ refers to the purely groundhook damping. In this study, the hybrid control results are obtained for $G_{hyb} = 60 \times 10^3$ and $\alpha = 0.55$.

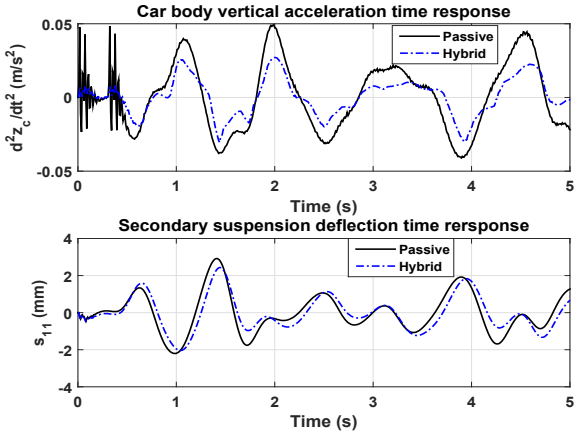


Fig. 12. The car body heave acceleration and the secondary suspension deflection time responses of the passive and hybrid controlled vehicle.

The Fig. 12 and Fig. 13 show the vehicle outputs time responses and the Table 1 lists the rms performances of skyhook, groundhook and the hybrid algorithms. According to the figures and table, the hybrid control performs best especially on reducing the vibration effects on car body. The groundhook damping is directly related with the unsprung mass (bogies) then according to the results it gives better results than the passive system on mini-

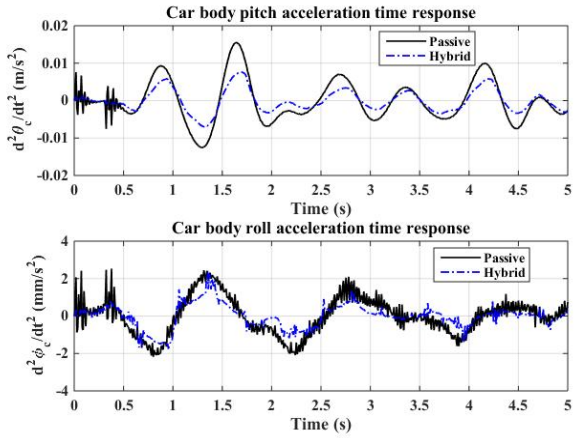


Fig. 13. The car body pitch and roll accelerations time responses of the passive and hybrid controlled vehicle.

mizing car body accelerations, but it could not reduce the secondary suspension travel.

In simulations, it is assumed that the absolute and relative velocities can be measured but in practice the velocities could not measured directly. In general, the accelerations are measured by the accelerometers and integrated then or the discplacements are measured by strain gages and differentiated then. This measurement methodology causes some problems in semi-active designs. Also, though the well results, since the semi-active force depends on the velocities of the sprung and unsprung masses, it has upper and lower bounds which restrict the performance.

Table 1. RMS performances of the vehicle outputs

| Output | Skyhook | Groundhook | Hybrid |
|---|---|---|---|
| $\ddot{z}_c$ | 29.4 | 4.96 | 44.4 |
| $\ddot{\theta}_c$ | 29.08 | 12.10 | 48.33 |
| $\ddot{\phi}_c$ | 20.32 | 2.76 | 37.8 |
| $s_{11}$ | 23.037 | -11.44 | 12 |

## 4. CONCLUSIONS

In this paper, motivated by the demand of energy saving, semi-active suspension control techniques have been studied for the secondary suspension variable dampers which are less energy-consumed compared to their active actuator counterparts. The classical s kyhook, ground hook and hybrid controls and their time responses have been plotted in order to gain a better understanding of their performances. The obtained results show that the skyhook control improves the ride comfort since it focuses on the vehicle body, while the groundhook control enhances the drive safety since it focuses solely on the bogie masses. The hybrid control offers the advantages of both latter methods which achieved a good compromise between ride comfort and drive safety.

The future work will focus on finding a remedy to improve the safety criteria of the comfort oriented semi-active suspension, by exploiting the LMI optimization and static output feedback control such that the rail holding criteria will not be deteriorated as well as the ride comfort criteria.

## REFERENCES

Foo, E. and Goodall, R.M. (2000). Active suspension control of felxible-bodied railway vehicles using electro-hydraulic and electro-magnetic actuators. *Control Engineering Practice*, 8, 507–518.

Guglielmino, E., Siretanu, T., Stammers, C.W., Ghita, G., and Giuclea, M. (2008). *Semi-Active Suspension Control-Improved Vehicle Ride and Road Friendliness*. Springer.

Hohenbichler, N., Six, K., and Abel, D. (2006). The benefit of skyhook control in high speed railway vehicles. In *4th IFAC Symposium on Mechatronic Systems*, 891–895.

Karnopp, D.C., Crosby, M.J., and Harwood, R.A. (1974). Vibration control using semi-active force generators. *Journal of ASME*, 96:2, 616–626.

Leblebici, A.S. and Türkay, S. (2016). The influence of passive suspension parameters on the ride performance of high speed passengerrailway vehicle. In *Turkish National Conference on Automatic Control (TOK2016)*. Eskisehir, Turkey.

Lei, X. (2017). *High Speed Railway Track Dynamics - Models, Algorithms and Applications*. Springer.

Li, H. and Goodall, R.M. (1999). Lienar and non-linear skyhook damping control laws for active railway suspensions. *Control Engineering Practice*, 7, 843–850.

Savaresi, S.M., Silani, E., Bittanti, S., and Porciani, N. (2003). On performance evaluation methods and control strategies for semi-active suspension systems. In *42nd IEEE Conference on Decision and Control*. Maui, Hawaii U. S. A.

Vassal, C.P., Sename, O., Dugard, L., Mendoza, R.R., and Flores, L. (2006). Optimal skyhook control for semi-active suspensions. In *4th IFAC Symposium on Mechatronic Systems*, 608–613.

Zheng, X. (2011). *Active Vibration Control of Flexible Bodied Railway Vehicles via Smart Structures*. Ph.D. thesis, Loughborough University.

Zolotas, A.C. and Goodall, R.M. (2018). New insights from fractional order skyhook damping control for railway vehicles. *Vehicle System Dynamics*, 56(11), 1658–1681.